JOURNAL OF MATERIALS SCIENCE 28 (1993) 3373–3384

Fracture toughness and fracture mechanisms of PBT/PC/IM blend

Part I *Fracture properties*

JINGSHEN WU, YIN-WING MAI, BRIAN COTTERELL
Centre for Advanced Materials Technology, Department of Mechanical Engineering, University of Sydney, Sydney, New South Wales 2006, Australia

The static and impact fracture toughnesses of a polybutylene terephthalate/polycarbonate/impact modifier (PBT/PC/IM) blend were studied at different temperatures. The static fracture toughness of the blend was evaluated via the specific fracture work concept and the J-integral analysis. A comparison of these two analytical methods showed that the specific essential fracture work, w_e, was equivalent to the J_{IC-81} obtained by the ASTM E813-81 procedure, representing the crack initiation resistance of the material. The discrepancy between w_e and J_{IC-89} of ASTM E813-89 was caused by the extra energy component in J_{IC-89} consumed by a 0.2 mm crack growth. Impact fracture toughness was also analysed using the specific essential fracture work approach. When the fracture was elastic, w_e was equivalent to the critical potential energy release rate, G_{IC}, obtained via LEFM analysis. Temperature and strain-rate effects on the fracture toughness were also studied. The increase in impact toughness with temperature was attributed to two different toughening mechanisms, namely, the relaxation processes of the rubbery particles and the parent polymers in a relatively low-temperature range and thermal blunting of the crack tip at higher temperatures. The enhancement in static fracture toughness at temperatures below $-60\,^{\circ}C$ was thought to be caused by plastic crack-tip blunting, but the monotonic reduction in yield stress was largely responsible for the toughness decreasing with higher temperatures. The temperature-dependent fracture toughness data obtained in static tests could be horizontally shifted to match roughly the data for the impact tests, indicating the existence of a time–temperature equivalence relationship.

1. Introduction

Linear elastic fracture mechanics (LEFM) is now widely used to characterize fracture behaviour of polymeric materials [1]. The size and geometry-independent parameters, K_{IC} and G_{IC}, have been proven to represent true material constants of most glassy polymers, provided that certain restrictive size criteria of the testing specimen have been satisfied [2] to meet the requirements of plane-strain fracture. For most homogeneous glassy polymers, such as polymethyl methacrylate (PMMA), polystyrene (PS) and high-density polyethylene (HDPE), these requirements are fairly easy to achieve. Previous work done by Chan and Williams [2] and Flueler *et al.* [3] shows that a valid HDPE sample for plane-strain K_{IC} test should be 10 mm thick and 20 mm wide, which are similar to the specimen size used for metal materials. But when toughened polymer blends are involved, because of their low yield stress and high toughness, application of the LEFM method very often requires an unrealistic specimen size to obtain a valid K_{IC} or G_{IC} value. For instance, a toughened nylon with $K_{IC} = 8.5\ MPa\,m^{1/2}$ and yield stress $\sigma_y = 50$ MPa requires a specimen at least 70 mm thick and 140 mm wide to generate a valid K_{IC}. These size requirements are now not easy to satisfy. This difficulty has led to the development of the J-integral analysis proposed by Rice [4]. The experimental procedure to determine the critical J-integral, J_{IC}, was later suggested by Begley and Landes by construction of the crack-growth resistance curve and crack-blunting line [5, 6]. Physically, the J-integral can be considered as the difference of the potential energy between two loaded identical bodies with slightly different crack lengths, i.e.

$$J = -\frac{1}{B}\frac{dU}{da} \tag{1}$$

where B is the thickness of the loaded body, U is the total potential energy which can be obtained by measuring the area under the load–displacement curve and a is the crack length. Sumpter and Turner later expanded the above equation and rewrote it as [7]

$$J = J_e + J_p \tag{2}$$

$$J = \frac{\eta_e U_e}{B(W-a)} + \frac{\eta_p U_p}{B(W-a)} \tag{3}$$

where J_e and J_p are the elastic and plastic components of the total J, respectively, and η_e and η_p are elastic and plastic factors corresponding to J_e and J_p. $(W - a)$ is the ligament length. In notched-bend specimens, when $0.4 < a/W$ and < 0.6 both η_e and η_p equal to 2 and Equation 3 is simplified to

$$J = \frac{2U}{B(W - a)} \tag{4}$$

The procedure for J_{IC} determination has been standardized by ASTM E813 [8–10]. There are several versions of the standard available, namely ASTM E813-81, ASTM E813-87 and ASTM E813-89. The major difference between ASTM E913-81 and E813-87,89 lies in the determination of acceptable data points for J–R curve construction and how to define the J_{IC} value on the J–R curve.

In ASTM E813-81 the J–Δa data points used to construct a J–R curve are those points located between two exclusion lines parallel to the blunting line (specified by $J = 2\Delta a^* \delta_y$) at crack growth $\Delta a = 0.006$ $(W - a)$ and $\Delta a = 0.06$ $(W - a)$, respectively. The valid data points are then linearly regressed to obtain the J–R curve and the crack initiation point is defined as the intersection of the J–R curve with the blunting line, which gives J_{IC}. However, ASTM E813-87 and E813-89 recommend to use two different exclusion lines to select valid J–Δa data points for J–R curve construction. The exclusion lines in these versions are also parallel to the blunting line but drawn from the positions of $\Delta a = 0.15$ and 1.5 mm, respectively. The power-law regression curve of the selected points is the J–R curve whose intersection with a 0.2 mm offset line gives a crack resistance, J_{IC}, corresponding to a crack growth $\Delta a = 0.2$ mm. Strictly this is *not* an initiation value.

J-integral analysis is now broadly accepted for fracture analysis of ductile metallic materials and it is also being gradually employed in the toughness evaluation of ductile polymer materials because of the much less stringent specimen size requirements. However, some aspects of the method still remain controversial. Hashemi and Williams [11] found that the linearity of the J–R curve for tough polymers could exist much greater than 6% of the ligament length; Huang and Williams observed no definitive evidence of dynamic effects when J-integral tests were carried out at a relatively high loading rate with toughened nylon [12]. The validity of determining crack initiation by the intersection of the J–R curve and the blunting line was also questioned by Narisawa and Takemori [13] who showed that the critical J-value for crack initiation could not be properly specified by the blunting line when toughened polymer blends were evaluated. The same conclusion was also reached by Swei *et al.* from their J-integral analysis with toughened polyethylene [14].

As an alternative to the J-integral method, the specific fracture work analysis which is experimentally simple and theoretically sound has been suggested for the determination of toughness of ductile materials [15–20]. The concept was originally developed by Cotterell, Mai and their co-workers [15–20] and applied to thin metal sheets. This was later extended to study the ductile fracture of polymers. When a crack in a ductile solid is being loaded, the plastic flow occurs in an outer plastic zone bordering the fracture process zone where fracture takes place (see Fig. 1). It is necessary to separate the total fracture energy, W_f, into two parts, W_e and W_p, which are the energies dissipated in the fracture process zone and the plastic zone, respectively. Thus,

$$W_f = W_e + W_p \tag{5}$$

$$W_f = W_e B(W - a) + \beta W_p B(W - a)^2 \tag{6a}$$

$$W_f = W_e + \beta W_p (W - a) \tag{6b}$$

where W_f is the specific total fracture work, W_e and W_p are the specific essential fracture work and specific plastic work, respectively; β is the plastic zone shape factor; B, W and a are thickness, width and initial crack length of specimen. W_e is a surface energy in terms of work per unit fracture surface area and W_p is a volume energy having a unit of work per unit volume of deformed material. Obviously, when W_f is plotted against $(W - a)$ according to Equation 6b and subsequently extrapolated to zero ligament length, W_e can be obtained from the intercept at the Y-axis and the slope of the straight line represents βW_p. Because the plastic zone shape factor, β, changes with specimen geometry and initial crack length, a straight line relationship between w_f and $(W - a)$ can only be achieved if geometric similarity is retained for all ligament lengths.

It has been shown [15, 16] that the specific essential fracture work is a material constant for a given sheet thickness. It represents the work required for crack initiation or, as the case may be, crack propagation. In

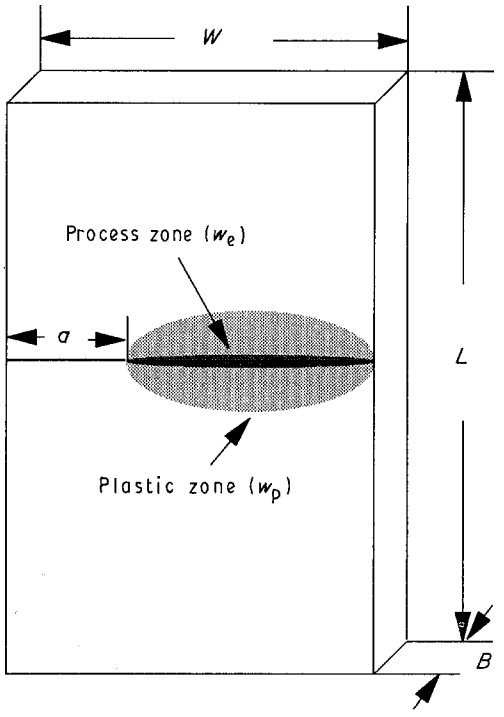

Figure 1 Schematic drawing of a ductile fracture specimen showing the inner fracture process zone and the outer plastic zone. w_e and w_p are the energies dissipated in these two zones.

addition, there is an equivalence between the specific fracture work, w_f, and the J-integral provided the J-controlled crack-growth conditions are satisfied, i.e.

$$w_f = J_R = J_C + \frac{dJ_R}{da}\Delta a \quad (7)$$

Comparing Equations 7 and 6b we obtain

$$w_e \equiv J_C \quad (8)$$

and

$$\beta w_p \equiv \alpha \frac{dJ_R}{da} \quad (9)$$

where α is a constant depending on the specimen geometry [16]. The above equivalent relationships have been confirmed for a range of ductile materials and several different specimen geometries. Thus, the specific fracture work technique can be used as an alternative to the J-integral analysis but it is much easier to perform experimentally.

Many polymer blends are designed to satisfy the increasing demands of high toughness at low temperatures and high strain rates [21–23]. Therefore, to characterize the toughness under impact conditions is particularly important. The conventional Charpy and Izod impact tests measure the total energy required for breaking a standard notched bar and the apparent surface fracture energy is then obtained by dividing the total energy over the ligament area. Unlike the critical potential energy release rate, G_{IC}, or J-integral, J_{IC}, the apparent surface fracture energy is normally not reproducible, specimen geometry and size dependent, and varies with testing method.

Analysis of impact energy data based on LEFM was derived by Marshall *et al.* [24] and Brown [25]. The impact toughness, in terms of G_{IC}, of an elastically fractured material can be successfully evaluated by breaking a series of specimens with different initial crack lengths. The impact fracture energy, U, measured is related to G_{IC} by [24]

$$U = G_{IC}BW\phi(a/W) + U_k \quad (10)$$

where a is the initial crack length, B and W are the thickness and width of specimen, respectively, and U_k is the kinetic energy loss. The correction factor, ϕ, is a function of a/W to account for geometry effects. Thus when U is plotted against $BW\phi$, a straight line with G_{IC} as the slope and U_k as the intercept can be obtained. Equation 10 has been successfully used to study the impact fracture behaviour of many brittle polymers. However, its application to ductile polymer blends is not tested.

The application of J-integral analysis to characterize the impact behaviour of ductile polymers has received some recent attention. Bramuzzo [26] investigated a series of rubber-toughened polypropylene by an instrumented impact tester together with a high-speed camera. However, the precise measurement of true crack extension in the specimen was difficult to obtain. Vu-Khanh also proposed a model to describe the fracture property of ductile polymers [27]. He obtained a straight-line relationship between the fracture energy and the fracture surface area, and further proposed that the tearing modulus [28, 29]

$$T = \frac{E}{\sigma_y^2}\frac{dJ_R}{da} \quad (11)$$

is a material constant. Criticisms of this model were given elsewhere [30], and in particular it was emphasized that T could not be constant in these testing conditions.

In the present study, the specific fracture work concept is employed to investigate both the static and impact fracture behaviours of a toughened polybutylene terephthalate (PBT)/polycarbonate (PC)/impact modifier (IM) blend at different temperatures. In Part I of this series of papers we describe the fracture toughness results. The static fracture toughness of the blend in terms of the specific essential fracture work, w_e, is compared to the J_{IC} values obtained via the J-integral methods of E813-81 and E813-89. The validity of the theoretical analysis and the effects of temperature and strain rate on the fracture toughness are discussed. The toughening mechanisms involved in both static and dynamic fractures are given in Part II [31].

2. Experimental procedure

2.1. Material and specimen preparation

The material used in this study was a commercial grade polybutylene terephthalate (PBT)/polycarbonate (PC)/impact modifier (IM) blend supplied by Bayer AG (Australia) in the form of pellets (Makroblend PR52). The original pellets were dried at 120 °C for 8 h before being injection moulded into plaques at 260 °C.

The specimens for Charpy impact and single-edge notched bend (SENB) tests were cut from the plaques into test bars 8.1 mm wide (W), 60 mm long (L) and 6 mm thick (B). All specimens were subsequently notched on one side using a guillotine-like apparatus with a razor blade driven by a screw with 1 mm pitch. To avoid plastic deformation at the crack tip the razor blade should be always fresh and the pushing speed as slow as practical. The normalized crack lengths (a/W) of the specimens were varied from 0.05–0.75. The dimensions of the SENB specimens for the J-integral tests were $6 \times 12 \times 70\ mm^3$. A deep notch with $a/W = 0.5$ was made in the centre of one side of the test bars using the same notching technique.

2.2. Mechanical tests

To study the specific work of fracture static (5 mm min^{-1}) three-point bend tests were carried out on an Instron test machine (Instron 4302) in the temperature range -196 to $+70$ °C. The test rig used was designed in accordance with the ASTM standard for J-integral test. A set of specimens with different initial crack lengths were loaded until total failure occurred. The load versus loading-point displacement curves were recorded by a X–Y plotter. The energy absorbed during fracture was regarded as the area

under the load–displacement curve, which was measured digitally by a computer. J-integral tests were conducted on three-point bend SENB geometry with multiple specimens on the same Instron 4302 with the same crosshead speed and at three different temperatures, e.g. 25, 50 and 70 °C. When the load–displacement curve reached a certain position where a required crack extension was attained, the specimen was unloaded, immersed in liquid nitrogen for 20 min and subsequently fast separated by a hammer and wedge. The length of the stress-whitening zone between the end of the notch and the commencement of the fast fracture was considered as the true crack extension which was measured by a travelling microscope.

Charpy impact tests were performed on a Zwick 5102 impact tester with single-edge notched specimens in the temperature range 100 – 196 °C. During the tests specimens with different initial crack lengths were either kept cold in a liquid nitrogen/ethanol bath or heated in an oven to the temperature required for at least 20 min. The specimens were then quickly mounted on the specimen holder and impacted immediately. The impact fracture energy was directly taken from the scale on the machine. The impact speed was 2.96 m s^{-1}.

3. Results and discussion

3.1. Specific work of fracture and J-integral tests

The specific fracture energies, w_f, obtained in the SENB tests at different temperatures are plotted against ligament lengths $(W - a)$ in Fig. 2a for temperatures above ambient and in Fig. 2b for sub-ambient temperatures according to Equation 6b. The scatter of the data points in Fig. 2a is very small and the linearity of the curves is extremely good, indicating that the plastic zone size increases in proportion to the ligament length. The specific essential fracture work, w_e, can be obtained easily by extrapolating the straight line relationship to zero ligament length. The specific plastic work, w_p, can also be easily determined from the slope of the lines. At sub-ambient temperatures the straight line relationship between w_f and $(W - a)$ still holds, but the scatter of the data points is relatively large, as shown in Fig. 2b. It is also clear that in the temperature range 25 to – 60 °C the slope of the lines decreases gradually with decreasing temperature, implying that βw_p is smaller at a lower temperature. Because w_p must increase with decreasing temperature this means that β or the plastic zone size must decrease with temperature. In fact, it is expected that at very low temperatures the plastic flow in the ligament is negligible (i.e. $\beta \to 0$) and a horizontal line is obtained when w_f is plotted against $(W - a)$. This means that $w_f = w_e$ under these conditions.

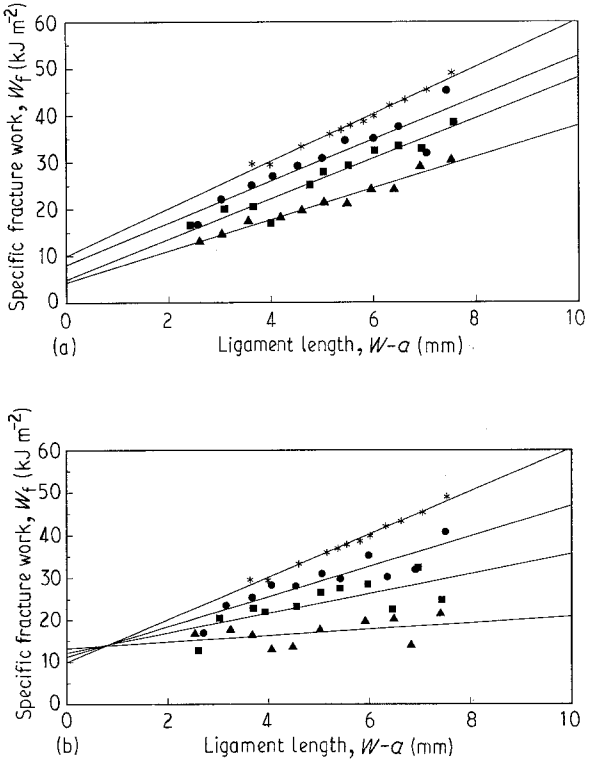

Figure 2 Plots of specific fracture work, w_f, against ligament length $(W - a)$ obtained in static bend tests at (a) $T \geq 25$ °C and (b) $T \leq 25$ °C. (a) (*) 25 °C, (●) 50 °C, (■) 70 °C, (▲) 100 °C. (b) (*) 25 °C, (●) 0 °C, (■) – 30 °C, (▲) – 60 °C.

The results of J-integral tests at three test temperatures are analysed according to ASTM E813-81 and E813-89, as shown in Fig. 3a–f. The information that emerged from these figures is similar to the findings published by Williams and co-workers [11, 12]. Firstly, the J–R curves obtained by the ASTM E813-81 procedure is linear far beyond the exclusion line of 6% ligament length. Secondly, there is little scatter in the data points used for construction of the J–R curve according to ASTM E813-89. Finally, the critical J-integral, J_{IC}, obtained by ASTM E813-81 (J_{IC-81}) are much smaller than the values derived from ASTM E813-89 (J_{IC-89}). This is simply because J_{IC-89} is the J value after a crack growth of 0.2 mm, whereas J_{IC-81} agree extremely well with those of w_e, suggesting that both J_{IC-81} and w_e give the crack initiation toughness. These experimental results also verified the equivalence of the two methods used and the validity of Equation 8.

The variation of w_e and J_{IC} with temperature is also shown in Fig. 4. The values of w_e for the tests performed at – 196 and – 100 °C are calculated from K_{IC} using $w_e = G_{IC} = K^2_{IC}/E$ because the fracture at these temperatures is totally elastic and LEFM is acceptable. There is a peak fracture toughness at about – 60 °C but on either side of this temperature the toughness decreases. This phenomenon is a result of two different toughening mechanisms involved. It is well known [21] that at low temperatures or high strain rates the controlling factor in toughening processes of a polymer blend is the relaxation behaviour of the rubbery particles. At a temperature below the glass transition temperature, T_g, of the rubber phase the rubbery particle acts only as a glassy filler having little or no effect on the parent polymers, and the blend behaves simply as a brittle polymer. The fracture toughness obtained at – 100 and – 196 °C confirms this conclusion.

When the temperature approaches T_g of the rubbery phase the relaxation of rubber becomes active

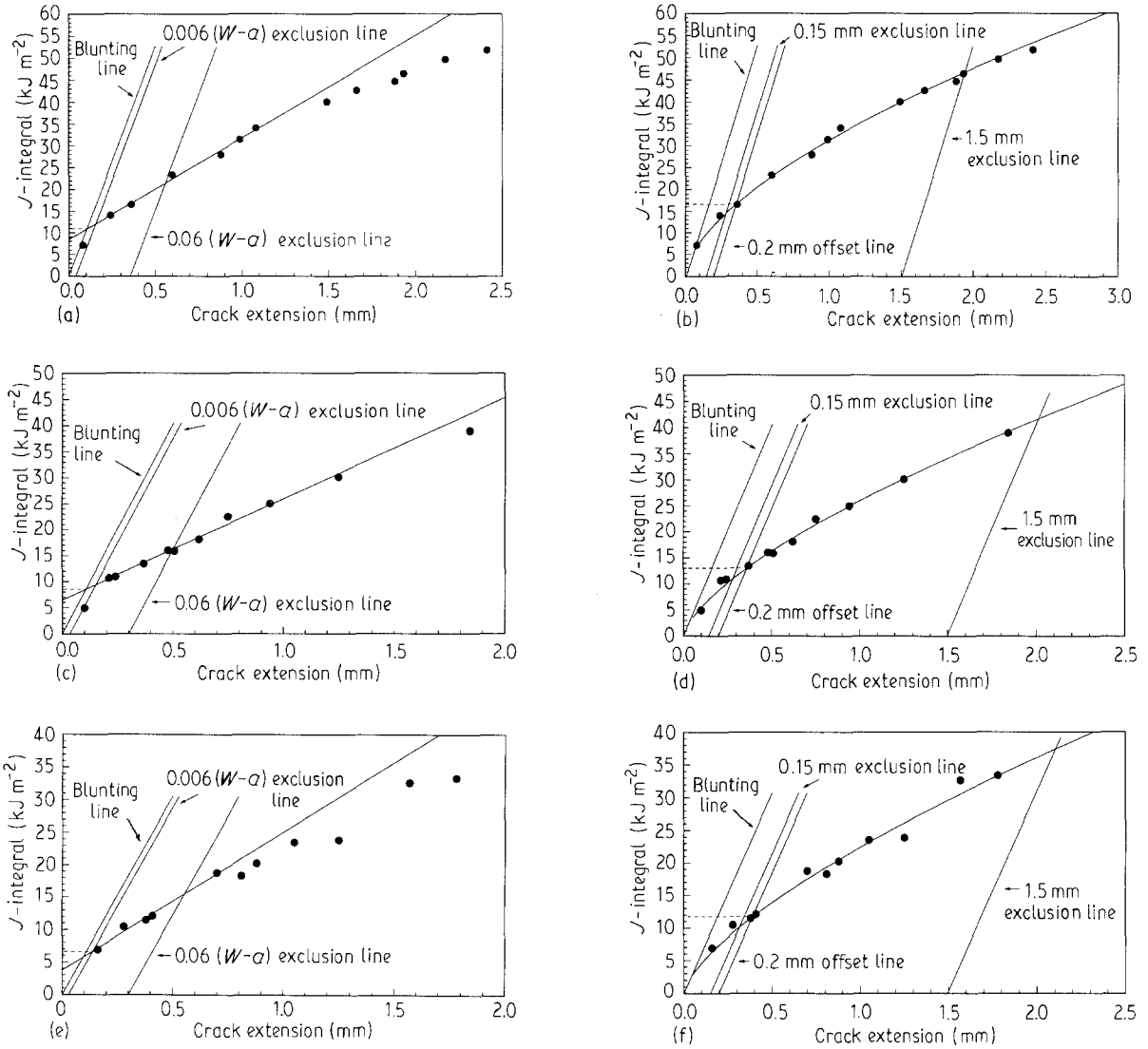

Figure 3 The *J–R* curves of PBT/PC/IM blend at different temperatures obtained via two standard testing methods; (a) 25 °C and ASTM E813-81, (b) 25 °C and ASTM E813-89, (c) 50 °C and ASTM E813-81, (d) 50 °C and ASTM E813-89, (e) 70 °C and ASTM E813-81, and (f) 70 °C and ASTM E813-89.

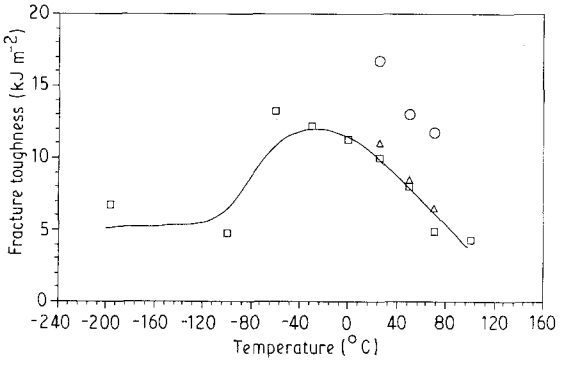

Figure 4 Variation of specific essential fracture work, w_e, with temperature in static bend tests. The comparison of (□) w_e and (△) J_{IC-81} and (○) J_{IC-89} is also shown.

and absorbs considerable energy. Because both PBT and PC possess a β relaxation peak at almost the same temperature (approximately − 70 °C) [32] as the T_g of rubber, a large amount of energy is also dissipated by the parent polymers [33, 34]. The combination of these two relaxation processes results in localized plastic deformation in the vicinity of the crack tip and it is this plastic blunting of the crack tip which leads to a dramatic increase in toughness within the temperature range − 100 to − 60 °C, as shown in Fig. 4.

With further increase in temperature there is a competition between the critical crack opening displacement (COD), δ_c, and the yield stress, σ_y. It is already established [1, 35] that $J_{IC} = \delta_c \sigma_y$ and both δ_c and σ_y are temperature-dependent [21]. If the decrease in yield stress outweighs the increase in COD the fracture toughness is reduced with temperature increase. In general, for many polymers, δ_c varies relatively little with temperature, hence the magnitude of fracture toughness is governed mainly by σ_y. Fig. 5 shows the yield stress of the blend plotted against temperature. Obviously, the monotonic reduction in σ_y with increasing temperature satisfactorily explains the decreasing fracture toughness found in the temperature range − 60–70 °C. A plot of fracture toughness against σ_y, Fig. 6, suggests that δ_c (the slope of the curve) is not a constant but increases with temperature.

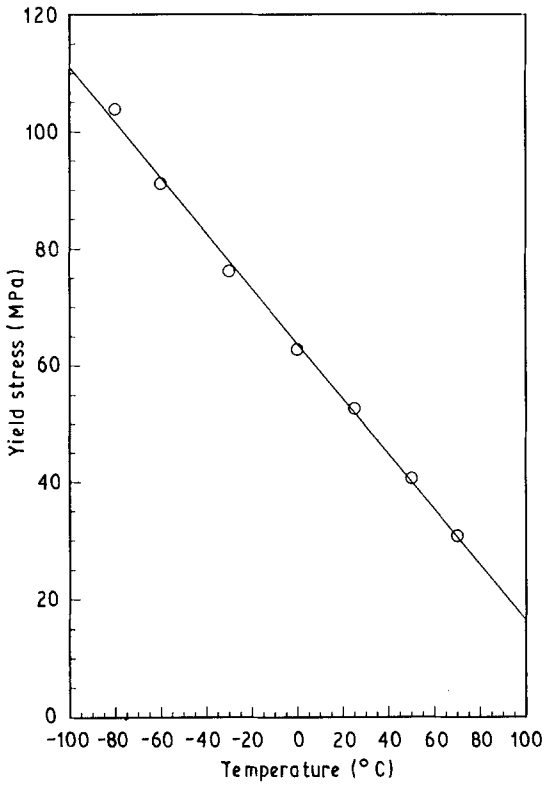

Figure 5 Variation of tensile yield stress, σ_y, with temperature in PBT/PC/IM blend at a deformation rate of 5 mm min^{-1}.

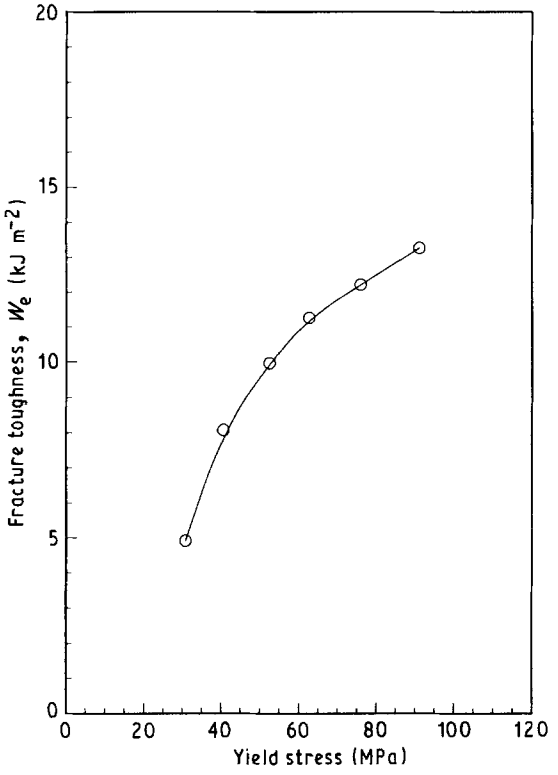

Figure 6 A plot of specific essential fracture work, w_e, against yield stress, σ_y.

3.2. Charpy impact tests

The Charpy impact results at different temperatures were first analysed with Equation 10. Plots of fracture energy, in terms of $U/(BW)$, against the calibration factor, ϕ, are shown in Fig. 7a–f. Clearly, when tested at a sufficiently low temperature, e.g. -196 and $-100\,^{\circ}C$, plastic flow is suppressed and the strain energy is stored in the sample elastically until G_{IC} is reached. In this case, elastic fracture occurs and Equation 10, based on LEFM, is valid. A straight-line relationship between $U/(BW)$ and ϕ is expected as shown in Fig. 7a and b. Hence, G_{IC} can be obtained from the slope of the lines which are 2.16 kJ m^{-2} at $-196\,^{\circ}C$ and 1.88 kJ m^{-2} at $-100\,^{\circ}C$. With rising temperature the effect of plastic deformation at the crack tip is not negligible and the $U/(BW)$–ϕ curves no longer obey Equation 10 as shown in Fig. 7c–f.

The same experimental data were then examined using the specific fracture work model. The fracture energy in terms of $U/B(W-a)$ is plotted against ligament length $(W-a)$ in Fig. 8a–e for tests performed below ambient temperature. As discussed in Section 3.1, when the tests are carried out at very low temperatures, a plateau value of $w_f = w_e$ is expected according to Equation 6b because of $\beta \to 0$. But all the curves in Fig. 8 have an upward curvature, even at -196 and $-100\,^{\circ}C$. This implies that in the specific fracture energy, w_f, there must be an energy component which is not plastic work but which increases with ligament length. Further tests at -100 and $-196\,^{\circ}C$ discovered that the kinetic energy involved in impact is the cause of the curvature. It is known that when an elastic body is subjected to impact there is kinetic energy absorption. This kinetic energy is greater when a more rigid body, for instance, a sample with a short crack or long ligament, is tested. Indeed, it was observed that the kinetic energy increases rather sharply with ligament length as shown in Fig. 9. Taking into account the kinetic energy, U_k, effect in Equation 6 we can rewrite

$$w_f = w_e B(W-a) + \beta w_p B(W-a)^2 + U_K \qquad (12a)$$

$$\frac{(w_f - U_k)}{B(W-a)} = w_e + \beta w_p (W-a) \qquad (12b)$$

Using Fig. 9 as the kinetic energy calibration curve and deducting U_k from w_f, $(w_f - U_k)/B(W-a)$ is replotted against $(W-a)$ for the test at -100 and $-196\,^{\circ}C$. As expected, the corrected specific fracture work is a straight horizontal line with $w_f = w_e$ for all ligament lengths, Fig. 8a and b. The large scatter is associated with the kinetic energy measurements. The values of w_e obtained in this way are 1.74 and 1.23 kJ m^{-2} at -196 and $-100\,^{\circ}C$, respectively. In fact, it is not always necessary to deduct U_k from w_f to obtain w_e. It is always possible to subtract the kinetic energy effect by extrapolating to zero $(W-a)$ because the kinetic energy drops down to zero at zero ligament length. Actually, the w_e values obtained by directly extrapolating to zero ligament, which are 2.08 kJ m^{-2} at $-196\,^{\circ}C$ and 1.43 kJ m^{-2} at $-100\,^{\circ}C$, are closer to the values obtained using Equation 10 based on Williams' model [36, 37] (i.e. 2.16 and 1.88 kJ m^{-2}) because the additional errors caused by U_k measurement are avoided.

With the increase of testing temperature, plastic flow at the crack tip becomes no longer negligible and

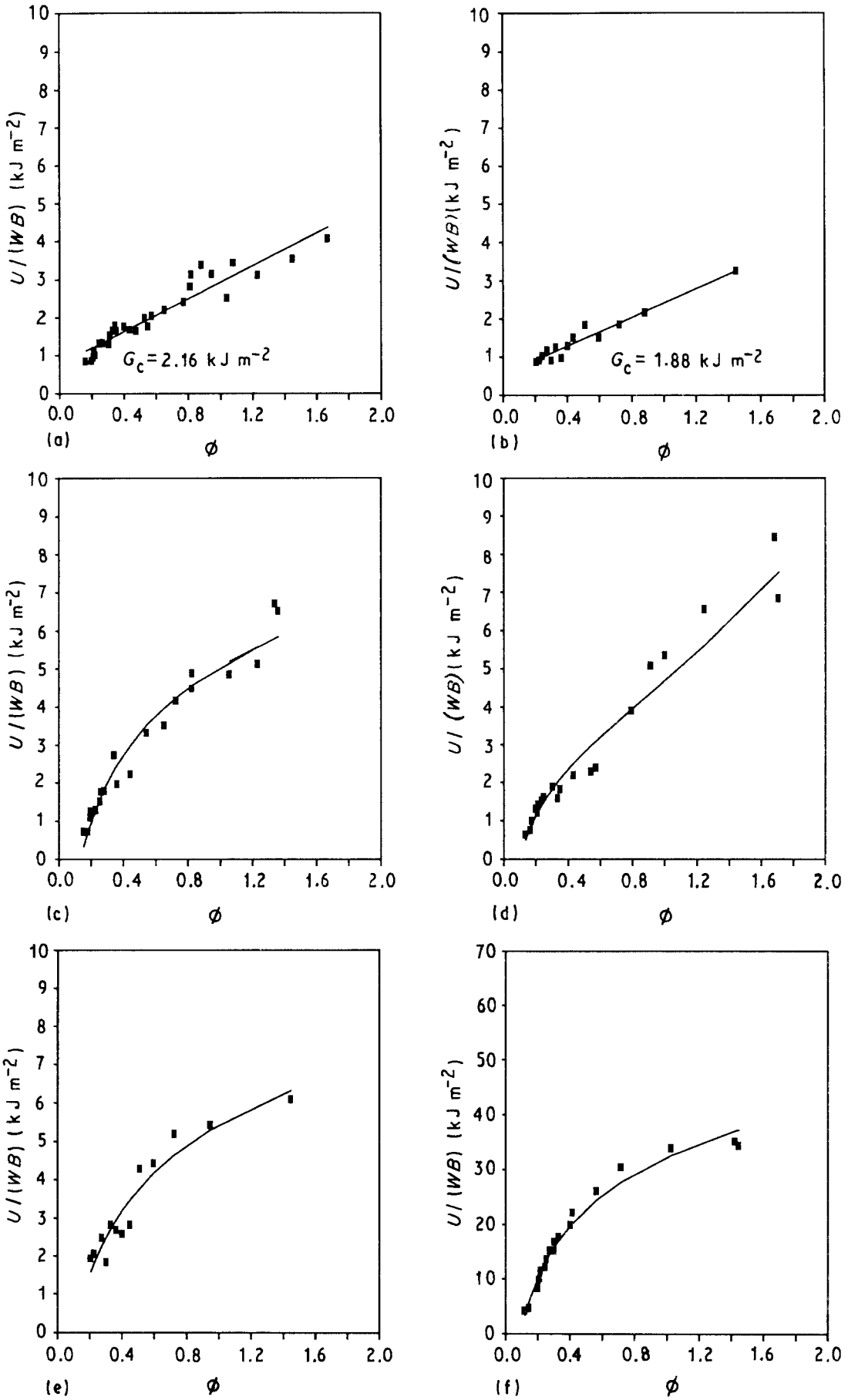

Figure 7 The relationship between the impact fracture energy (U/BW), and geometry correction factor, ϕ, obtained by Williams' model [24] at different temperatures. T: (a) $-196\,^{\circ}C$, (b) $-100\,^{\circ}C$, (c) $-60\,^{\circ}C$, (d) $-30\,^{\circ}C$, (e) $0\,^{\circ}C$, (f) room temperature.

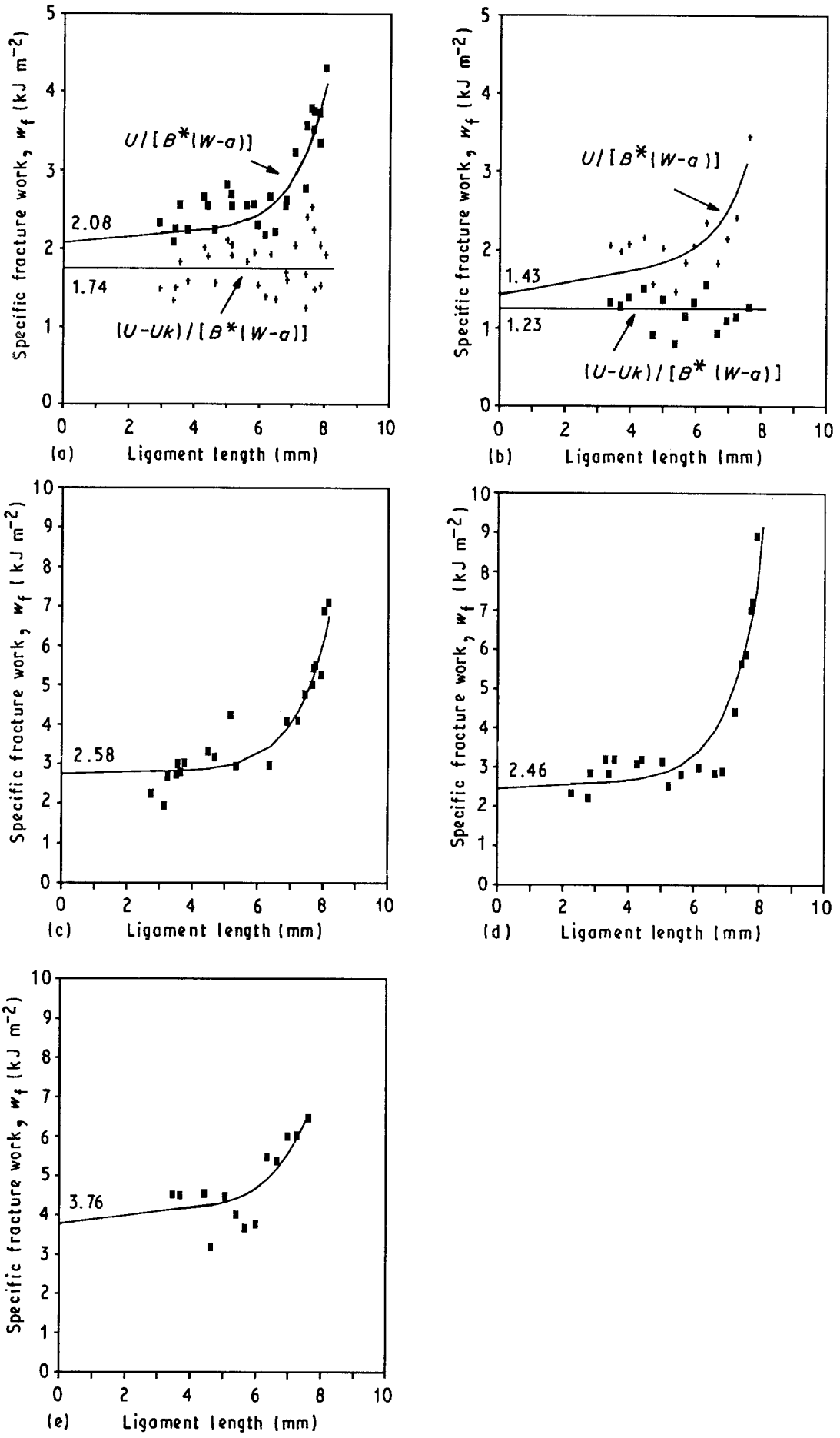

Figure 8 Plots of impact fracture energy in terms of specific fracture work, w_f, against ligament length ($W - a$), obtained at sub-ambient temperatures. T: (a) − 196 °C, (b) − 100 °C, (c) − 60 °C, (d) − 30 °C, (e) 0 °C.

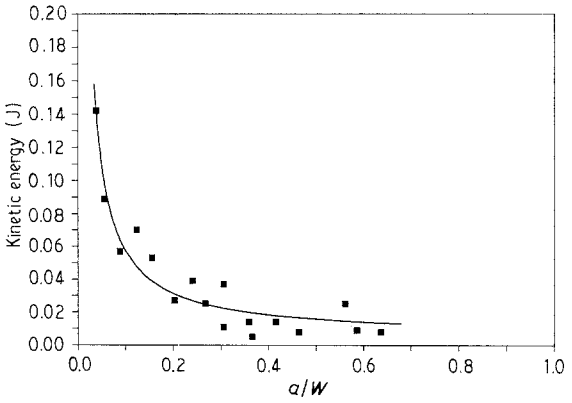

Figure 9 Variation of kinetic energy with ligament length at − 196 °C.

fracture becomes progressively semi-brittle and semi-ductile. The kinetic energy effect is vanishing but the energy dissipation due to plastic deformation is, however, becoming more and more dominant. The second term on the right in Equation 12b, $\beta w_p(W - a)$, is no longer zero as long as the ligament length is not zero. The upward curvature in the data shown in Fig. 8c–e in the temperature range − 100–25 °C is now a result of a mixed effects of U_k and w_p. However, because both U_k and w_p tend towards zero at zero ligament length, it is still possible to obtain w_e from the intercept by extrapolating to the zero ligament length. The specific plastic work, w_p, is not available because w_p and U_k cannot be separated easily.

When the temperature for complete ductile stable fracture is reached, the kinetic energy becomes negligible compared with the total energy absorbed and Equation 6b holds. In Fig. 10d the data obtained at room temperature do give a straight-line relationship with $w_e = 9.14\ \text{kJ m}^{-2}$ and $\beta^* w_p = 3.64 \times 10^3\ \text{kJ m}^{-3}$. However, at higher temperatures the data do not give a linear relationship. The slope of the curves increases when a critical ratio of $a/W \approx 0.2$ is reached, as shown in Fig. 10a–c. This implies that either β or w_p or both increase with ligament length.

It is known from the results of our earlier work [38, 39] that a notched specimen with a shallow crack (small a/W ratio) provides less plastic constraint at the crack tip than a deeply notched specimen. There is a transition a/W ratio at which a sharp change in plastic constraint occurs. For a sharp-notched three-point bend specimen, this transition occurs at $a/W = 0.177$ [39]. It is therefore reasonable to expect an increase in βw_p for $a/W \leq 0.2$ due to the increase in plastic zone size. However, β is not invariant with ligament length. If we define $h[= \beta(W - a)]$ as an effective depth of the plastic zone (as sketched in Fig. 11) then a straight-line relationship between w_f and h should hold, provided that w_p is a constant. In this work the effective plastic zone depth was measured using a cold-section technique [40] and an optical microscope. The stress-whitening area, A, on the sub-fracture surface was regarded as the plastic zone area and was measured digitally. h is then obtained by dividing A with $(W - a)$. Fig. 12a–c show the expected straight-line correlations between w_f and h for all tests at high temperatures. It suggests that w_p is a constant and does not change with crack length. The intercept again gives the specific essential fracture work, w_e,

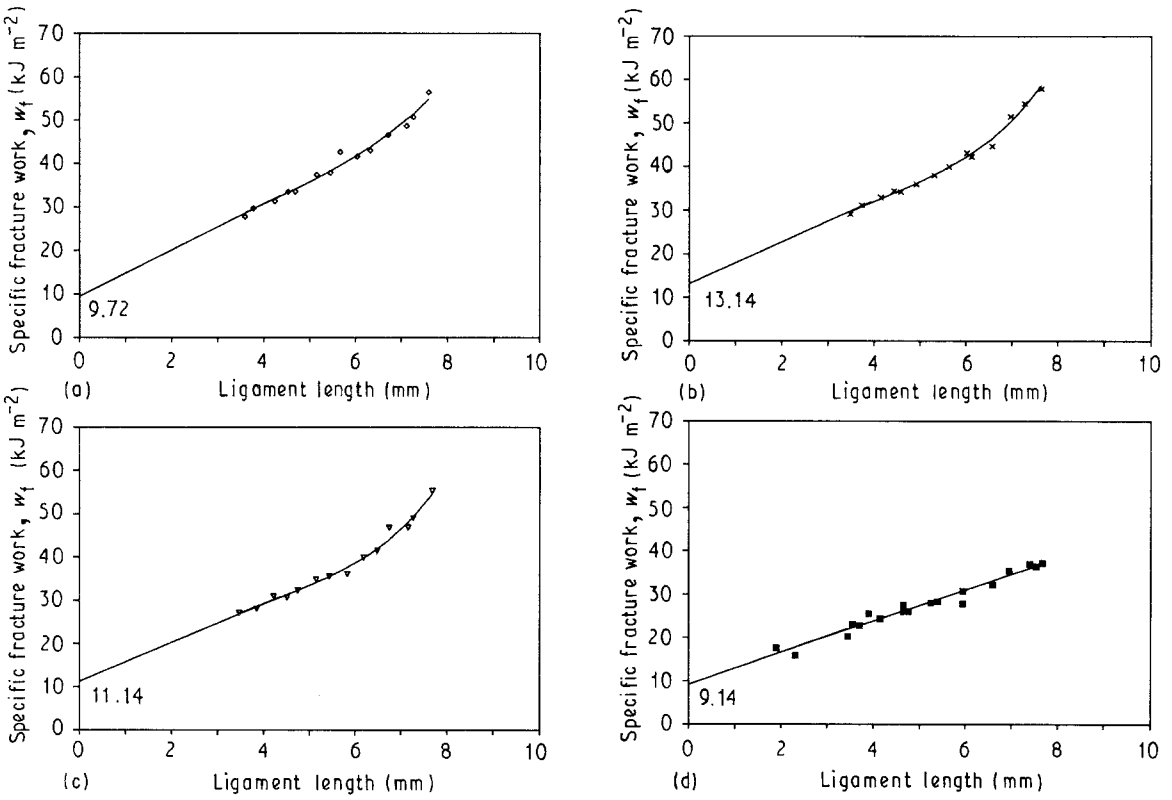

Figure 10 Plots of specific fracture work, w_f, versus ligament length $(W - a)$, obtained at temperatures above ambient: (a) 100 °C, (b) 70 °C, (c) 50 °C, (d) room temperature.

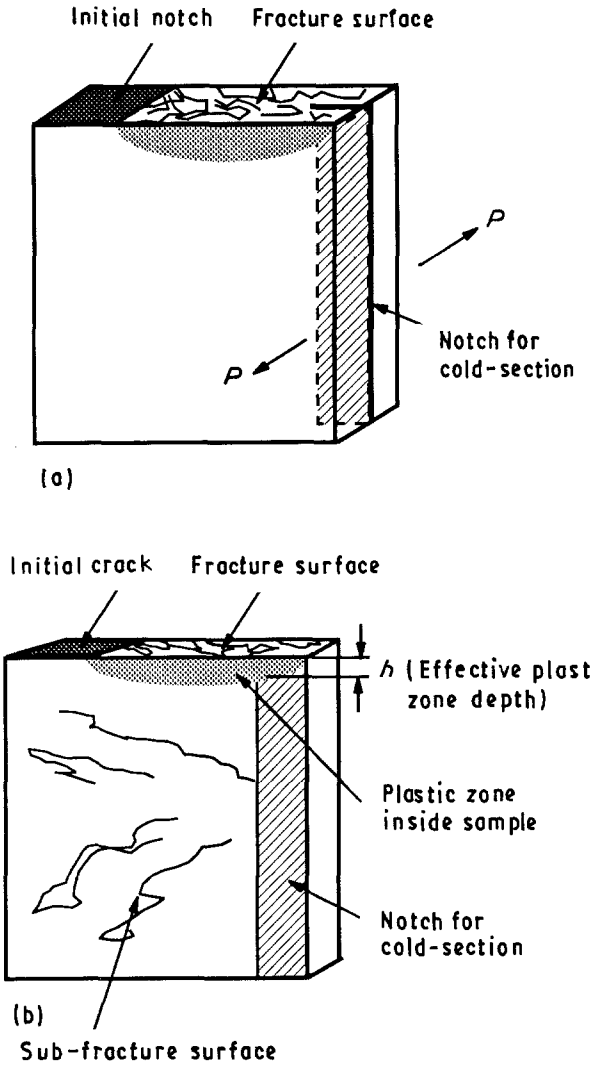

Figure 11 Sketches showing (a) the cold-section process and (b) effective stress-whitening zone depth, h.

which is quite close to that obtained by extrapolating the linear part of the w_f versus $(W - a)$ curves in Fig. 10a–c to zero ligament length.

The variation of w_e with temperature is shown in Fig. 13. Briefly, w_e is constant from -196 to $-100\,^{\circ}C$, increases slightly in the temperature range -100 to $-30\,^{\circ}C$, rises dramatically from -30–$70\,^{\circ}C$, and then drops down between 70 and $100\,^{\circ}C$.

The temperature effect on the impact fracture toughness of polymeric materials has received a good deal of attention in the past [41–47]. Much of the work has been concentrated on the question of whether or not the molecular relaxation processes occurring in a polymer have a one-to-one correlation with the energy absorption mechanisms observed in the mechanical tests. Though the answer to this question is still far from settled, however, with the aid of previous work, the experimental observations of the present study are not very difficult to understand. As pointed out in a previous paper [46], there are two factors which are of particular importance when the temperature effect on the impact behaviour is considered, i.e. the tan δ loss and the crack-tip thermal blunting caused by adiabatic heating induced by the high strain rate in an impact test. Normally, tan δ has a less pronounced effect on the energy absorption process than that of crack-tip blunting. It is therefore expected that tan δ loss becomes operative only when the effective temperature of the local material at the crack tip, which is equal to the test temperature plus the temperature increase due to adiabatic heating, is lower than the softening temperature of the blend. According to our DSC study of the PBT/PC/IM blend, it is found that there is a β transition loss process with a peak at about $-70\,^{\circ}C$. On the other

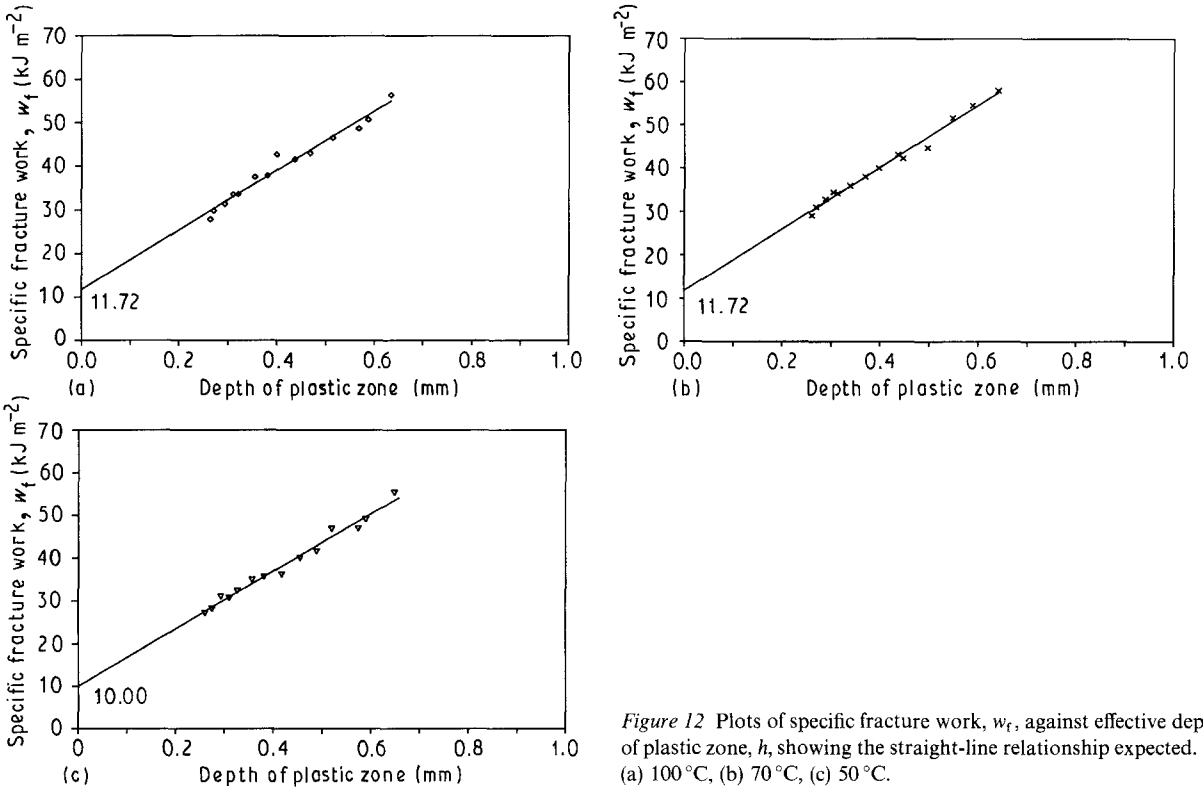

Figure 12 Plots of specific fracture work, w_f, against effective depth of plastic zone, h, showing the straight-line relationship expected. T: (a) $100\,^{\circ}C$, (b) $70\,^{\circ}C$, (c) $50\,^{\circ}C$.

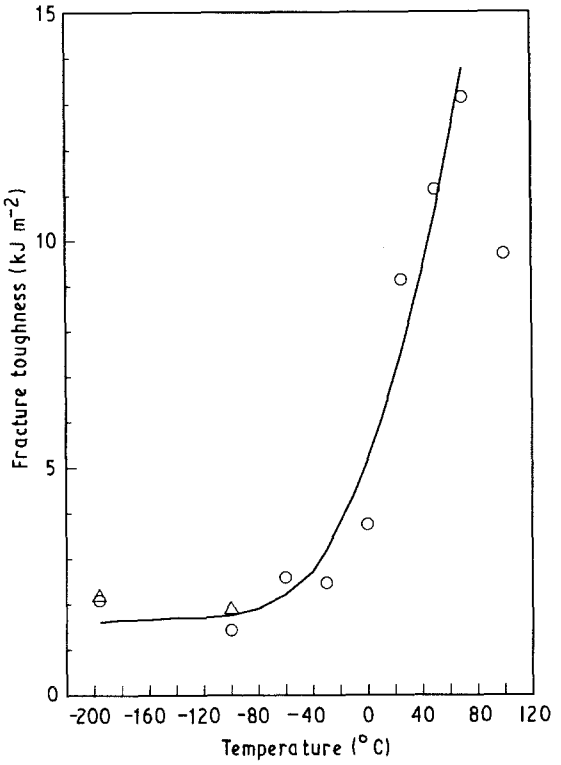

Figure 13 Variation of impact fracture toughness in terms of (○) specific essential fracture work, w_e, with test temperature. (△) Toughness values, G_c, obtained from Equation 10.

hand, the effective temperature of the local material, T_e, in the crack-tip region can be estimated by [48]

$$T_e = T + \Delta T \tag{13}$$

where T is the test temperature and ΔT is the temperature increase which can be calculated from

$$\Delta T = \frac{w_e}{(\pi \rho c k t)^{\frac{1}{2}}} \tag{14}$$

The data supplied by the manufacturer give the density $\rho = 1.23 \times 10^3$ kJ m^{-3}, specific heat $c = 1.18$ kJ kg^{-1} K^{-1}, thermal conductivity $k = 0.2 \times 10^{-3}$ kJ s^{-1} K^{-1} m^{-1}, and softening temperature $T_s = 150$ °C.

The loading time, t, in these tests is approximately 0.4 ms. At − 20 °C, where w_e is about 3.60 kJ m^{-2}, ΔT calculated from Equation 14 is approximately 188 °C and T_e is 168 °C which is just above the softening temperature, 150 °C. Therefore, thermal blunting becomes effective at about − 20 °C. Recall that the peak of β transition occurs at − 70 °C, we may conclude that (a) when the blend is tested at temperatures below − 100 °C, because there is no extra energy absorption process to occur, w_e equals G_{IC}; (b) in the temperature range − 100 to − 30 °C the slight increase in impact strength is a result of tan δ loss; (c) at temperatures higher than − 30 °C, the enhancement in impact toughness is solely caused by the crack-tip thermal blunting effect due to the adiabatic heating. The extent of the thermal crack blunting is amplified with increasing test temperature, leading to a steady increase in toughness. However, when the temperature at which the blend starts to lose its strength is reached, a reduction in toughness occurs and this happens at about 100 °C, as shown in Fig. 13.

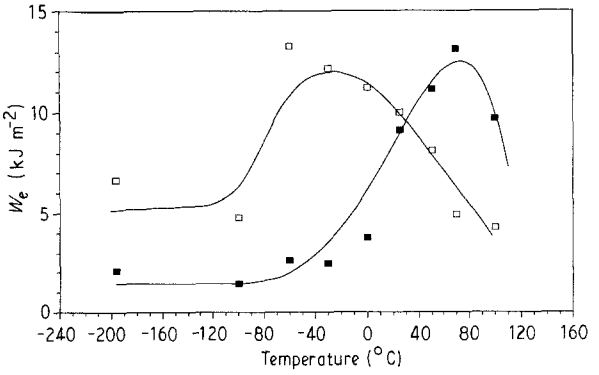

Figure 14 Comparison of the variations of fracture toughness, w_e, with temperature for both (□) static and (■) impact fracture tests.

Strain rate has a significant effect on the fracture toughness of many polymers and it has been investigated extensively by Yamini and Young [42], Kinloch *et al.* [43, 44], Williams and co-workers [45, 46] and Low and Mai [47] at different testing conditions. In general, the fracture toughness of polymers depends upon strain rate and temperature and there is a general equivalence between these two factors. The fracture behaviour observed at low temperatures and high strain rates can be reproduced at high temperatures with low strain rates. This behaviour is known as the time–temperature superposition [49]. Comparisons of the two sets of w_e values obtained in the same temperature range but with two different strain rates (5 mm min^{-1} and 2.96 m s^{-1}) are given in Fig. 14. The time–temperature superposition behaviour is obvious. If the curve representing the impact tests is shifted to the left along the temperature axis it is found that the results in the temperature range − 60–70 °C have the same trend as the static w_e results in the temperature range − 100 to − 60 °C. This suggests that the fracture behaviour observed in impact tests at a relatively high-temperature range is similar to that obtained in the static fracture tests but carried out in a low-temperature domain.

4. Conclusions

1. The specific fracture work concept can be applied to characterize the fracture behaviour of toughened polymer blends. The specific essential fracture work, w_e, is equivalent to the J_{IC} value obtained via ASTM E813-81, representing the crack initiation resistance of the material tested. The discrepancy between w_e and J_{IC} determined by ASTM E813-89 is caused by the extra energy dissipation in J_{IC-89} by a 0.2 mm crack growth.

2. The concept of specific fracture work developed with static tests has been successfully extended to impact tests. The upward curvature found on the w_f versus $(W - a)$ curves is caused by the kinetic energy dissipation when the fracture is completely elastic. When the fracture is entirely ductile the curvature on the curve is due to a drastic increase in the plastic zone size at a critical a/W ratio. However, in both cases, the specific essential fracture work, w_e, can always be

obtained by extrapolating the w_f versus $(W - a)$ curve to zero ligament length.

3. Testing temperature affects markedly the fracture toughness of the polymer blend tested. The static fracture toughness increases with temperature between -196 and $-60\,^{\circ}C$ as a result of the plastic blunting of the crack tip caused by the relaxation of rubbery particles at T_g, and β transition loss process of the parent polymers. The decrease of toughness at temperatures higher than $-60\,^{\circ}C$ is solely a consequence of the reduction of yield stress with temperature.

The impact fracture toughness increases monotonically with temperature until about $100\,^{\circ}C$. Because of the high strain rate, the relaxation processes of rubber and matrix can only contribute very slightly towards the toughness of the blend. However, when the effective temperature at the crack tip reaches the the softening temperature of the blend due to adiabatic heating there is a dramatic increase in fracture toughness caused by thermal blunting.

4. Strain rate has a strong influence on the fracture toughness of the polymer blend. The relationship between fracture toughness and temperature observed in the impact tests at high temperatures is equivalent to that in the static tests at low temperatures indicating the existence of a time–temperature equivalence.

Acknowledgements

We thank Bayer AG (Australia) for the supply of materials for testing. The financial support of a Sydney University Postgraduate Research Award to one of us (J. S. Wu) is greatly appreciated. We also thank the Sydney University Electron Microscope Unit for assistance in the use of their facilities.

References

1. J. G. WILLIAMS, "Fracture Mechanics of Polymers" (Ellis Horwood, Chichester, 1984).
2. M. K. V. CHAN and J. G. WILLIAMS, *Polym. Engng Sci.* **21** (1981) 1019.
3. P. FLUELER, D. R. ROBERTS, J. F. MANDELL and F. J. McGERRY, ASTM STP 736 (American Society for Testing and Materials, Philadelphia, PA, 1981) p. 15.
4. J. R. RICE, *J. Appl. Mech.* **35** (1968) 379.
5. J. A. BEGLEY and J. D. LANDS, in "Fracture Toughness", ASTM STP 514 (American Society for Testing and Materials, Philadelphia, PA, 1972) pp. 1–20.
6. J. D. LANDS and J. A. BEGLEY, *ibid.*, p. 24.
7. J. D. SUMPTER and C. E. TURNER, *Int. J. Fract.* **9** (1973) 320.
8. ASTM Standard E813-81, 1981 Annual Book of ASTM Standards, Part 10 (American Society for Testing and Materials, Philadelphia, PA, 1981) p. 810.
9. ASTM Standard E813-87, 1987 Annual Book of ASTM Standards, Part 10 (American Society for Testing and Materials, Philadelphia, PA, 1987) p. 1968.
10. ASTM Standard E813-89, 1989 Annual Book of ASTM Standards, Part 10 (American Society for Testing and Materials, Philadelphia, PA, 1989) p. 700.
11. S. HASHEMI and J. G. WILLIAMS, *Polymer* **27** (1986) 384.
12. D. D. HUANG and J. G. WILLIAMS, *J. Mater. Sci.* **22** (1987) 2503.
13. I. NARISAWA and M. T. TAKEMORI, *Polym. Engng Sci.* **29** (1989) 671.
14. H. SWEI, B. CRIST and S. H. CARR, *Polymer* **32** (1991) 1440.
15. Y.-W. MAI and B. COTTERELL, *Int. J. Fract.* **32** (1986) 105.
16. Y.-W. MAI, in Proceedings of International Symposium on "How to improve the toughness of polymers and composites", Yamagata University, Yamagata, Japan, 8 October 1990, pp. 138–45.
17. B. COTTERELL and J. K. REDDELL, *Int. J. Fract.* **13** (1977) 267.
18. Y.-W. MAI and B. COTTERELL, *Engng Fract. Mech.* **21** (1985) 123.
19. B. COTTERELL, E. LEE and Y.-W. MAI, *Int. J. Fract.* **20** (1982) 243.
20. Y.-W. MAI and B. COTTERELL, *J. Mater. Sci.* **15** (1980) 2296.
21. C. B. BUCKNALL, "Toughened Plastics" (Applied Science, London, 1977).
22. A. S. WOOD, *Modern Plastics* April (1985) 81.
23. K. WEIRAUCH, *Kunststoffe* **75** (1985) 700.
24. G. P. MARSHALL, J. G. WILLIAMS and C. E. TURNER, *J. Mater. Sci.* **8** (1973) 949.
25. H. R. BROWN, *J. Mater. Sci.* **8** (1973) 941.
26. M. BRAMUZZO, *Polym. Engng Sci.* **29** (1989) 1077.
27. T. Vu-KHANH, *Polymer* **29** (1988) 1979.
28. P. C. PARIS, H. TADA, A. ZAHOOR and H. ERNST, in ASTM STP 668 (American Society for Testing and Materials, Philadelphia, PA, 1979) p. 5.
29. A. ZAHOOR and P. C. PARIS, *J. Eng. Mater. Tech.* **103** (1981) 46.
30. Y.-W. MAI, *Polym. Commun.* **30** (1989) 330.
31. J. S. WU and Y.-W. MAI, *J. Mater. Sci.* **28** (1993)
32. D. C. WAHRMUND, D. R. PAUL and J. W. BARLOW, *J. Appl. Polym. Sci.* **22** (1978) 2155.
33. G. P. MARSHALL, L. H. COUTTS and J. G. WILLIAMS, *J. Mater. Sci.* **9** (1974) 1409.
34. M. PARVIN and J. G. WILLIAMS, *ibid.* **10** (1975) 1883.
35. F. M. BURDEKIN and D. E. W. STONE, *J Strain Anal.* **1** (1966) 145.
36. M. W. BIRCH and J. G. WILLIAMS, *Int. J. Fract.* **14** (1978) 69.
37. E. PLATI and J. G. WILLIAMS, *Polym. Engng Sci.* **15** (1975) 470.
38. S.-X. WU, Y.-W. MAI and B. COTTERELL, *Int. J. Mech. Sci.* **29** (1987) 557.
39. S.-X. WU, PhD thesis, The University of Sydney, Sydney, Australia (1990).
40. F. SPERONI, E. CASTOLDI, P. FABBRI and T. CASIRAGHI, *J. Mater. Sci.* **24** (1989) 2165.
41. P. I. VINCENT, *Polymer* **15** (1974) 111.
42. S. YAMINI and R. J. YOUNG, *ibid.* **18** (1977) 1075.
43. A. J. KINLOCH, S. J. SHAW, D. A. TOD and D. L. HUNSTON, *ibid.* **24** (1983) 1341.
44. *Idem, ibid.* **24** (1983) 1355.
45. M. KISBENYI, M. W. BIRCH, J. M. HODGKINSON and J. G. WILLIAMS, *ibid.* **20** (1979) 1289.
46. E. PLATI and J. G. WILLIAMS, *ibid.* **16** (1975) 915.
47. I.-M. LOW and Y.-W. MAI, *J. Mater. Sci.* **24** (1989) 1634.
48. J. G. WILLIAMS and J. M. HODGKINSON, *Proc. R. Soc. Lond.* **A375** (81) 231.
49. A. J. KINLOCH and R. J. YOUNG, "Fracture Behaviour of Polymers" (Applied Science, London, 1983).

Received 21 October
and accepted 19 November 1992